Research papers

Dating dry-stone walls with rock surface luminescence: A case study from the Italian Alps

Lucas Ageby [a],[*], Diego E. Angelucci [b], Dominik Brill [a], Francesco Carrer [c], Helmut Brückner [a], Nicole Klasen [a]

[a] *Institute of Geography, University of Cologne, 50923 Cologne, Germany*
[b] *Dipartimento di Lettere e Filosofia, University of Trento, 38122 Trento, Italy*
[c] *School of History, Classics and Archaeology, Newcastle University, NE1 7RU, Newcastle, UK*

ARTICLE INFO

ABSTRACT

Dating the construction of dry-stone walls is challenging since such structures are typically built without any mortar that can be used for dating. Rock surface luminescence dating is a developing dating method that could advance chronological insights from structures constructed using dry-stone techniques. This study explores rock surface luminescence dating by targeting dry-stone walls from two enclosure complexes and a hut located in the pastoral upland landscape in Val di Sole, Italy. Gneissic rocks were collected from the dry-stone walls, including surfaces that were either exposed or covered (buried) during the time of sampling. Their respective exposure and burial histories were investigated by measuring the luminescence intensity in feldspar minerals from polymineral rock slices. From covered rock surfaces from one enclosure complex, we calculated recent burial ages (∽200 a) from one rock, and burial of ∽500 a (bottom surface) and 3750 ± 660 a (top surface) from a second rock. The top surfaces of two additional rocks date the construction of an adjacent hut to the Early Middle Ages. The luminescence-depth profile from one such rock has a complex exposure and burial history, including events that predate the hut's construction. Fitted exposure ages from a second enclosure complex suggest with significant errors either a recent age (<10 a) or construction during the 19th century AD. Burial dating using rock surface luminescence dating appears feasible for dry-stone walls provided that the rock surface was sufficiently exposed before being incorporated into the structure; here, the gneissic surfaces were bleached to depths of ∽0-2 mm before the last burial. Contrariwise, exposure dating generally underestimates the expected age. The variation in ages observed from our rock surfaces indicates that the degree of preservation of the wall, the position of the rock, erosion, and knowledge regarding the general archaeological setting are essential to interpreting the estimated ages. In this study, rock surface luminescence dating provides new, previously inaccessible chronological data with implications for interpreting human activities in the alpine areas of Val di Sole.

1. Introduction

The construction of dry-stone structures began early in the history of humankind. The most ancient dry-stone walls date from the Palaeolithic (e.g., Jaubert et al., 2016; Yar and Dubois, 1996). Since the Neolithic (e.g., Holl, 1998; Mazet, 2006), dry-stone structures were built to support functions related to animal husbandry. Later on, dry-stone masonry remained an established construction technique for dwellings (e.g., Ferrater et al., 2015; Manley, 1990), fences and enclosures (e.g., Colominas et al., 2020; Kremenić et al., 2021; Walsh et al., 2014), as well as fortifications (e.g., Levine et al., 2019; Liszka, 2017) throughout history.

Due to the common historical use of dry-stone walls, methods to directly date the construction of dry-stone walls are critically important. Since dry-stone walls typically lack mortar, numerical dating of such structures is usually accomplished using radiocarbon dating of organic material recovered from associated archaeological layers (e.g., Ilves, 2018; Manley, 1990; Passariello et al., 2010; Walsh, 2005) once stratigraphic correlation has been assessed through the standard methods of archaeological stratigraphy (Harris, 1989). While essential in many archaeological settings, this approach does not directly date the actual construction of the structures. Also, not all such structures have associated archaeological horizons or assemblages, or the record might

* Corresponding author.
 E-mail address: lageby@uni-koeln.de (L. Ageby).

not be stratigraphically associated with the time of construction. An additional method to date the age of dry-stone structures is luminescence dating of sediment grains trapped between the stones (Junge et al., 2016; Kemp et al., 2022), grains from the soil beneath the positioned stones (Sohbati et al., 2015; Vafiadou et al., 2007). However, alternative approaches are necessary for stone structures where trapped grains are not available.

Developments in luminescence dating – applied to rock surfaces – potentially provide a dating method that could be used for dry-stone walls. Rock surface luminescence dating is a dating technique (e.g., Habermann et al., 2000; Liritzis et al., 2019b,a; Sohbati et al., 2011, 2012a,b; Vafiadou et al., 2007), that enables dating of exposed (e.g., Brill et al., 2021; Gliganic et al., 2019; Lehmann et al., 2018; Polikreti et al., 2002; Sohbati et al., 2011, 2012b) and buried (e.g., Gliganic et al., 2021; Ishii et al., 2022; Rades et al., 2018; Sohbati et al., 2012a, 2015) rock surfaces. The basis of the method is that the luminescence signal intensity decreases into the rock during periods of exposure (bleaching) and increases during periods of burial. If the lithology is sufficiently translucent to allow for bleaching to occur (Ou et al., 2018), then minutes to hours of exposure can be enough to bleach the luminescence signal in the surface grains in some lithologies (Sohbati et al., 2011; Vafiadou et al., 2007), and prolonged exposure gradually resets the signal deeper into the rocks (e.g., Gliganic et al., 2019; Laskaris and Liritzis, 2011; Ou et al., 2018; Polikreti et al., 2002; Sohbati et al., 2011). The duration of exposure for a rock surface can be constrained if the bleaching rate of the signal is known (e.g., Sohbati et al., 2012b). The bleaching rate depends on the lithology, the photoionisation cross-section of the electron traps, and the photon flux at the rock surface (Sohbati et al., 2011) — parameters that vary between different samples and sites. Using locally sourced calibration samples with known exposure histories can constrain the mentioned parameters, after which the exposure time can be calculated for surfaces with unknown exposure histories for absolute dating (Brill et al., 2021; Gliganic et al., 2019; Lehmann et al., 2018; Sohbati et al., 2012b), or for artefact authentication (Polikreti et al., 2002). Burial ages can be extracted from rock surfaces if burial events can be identified by the presence of luminescence signal intensity plateaus that are not in field saturation (e.g., al Khasawneh et al., 2019a; Freiesleben et al., 2015; Gliganic et al., 2021; Jenkins et al., 2018; Liritzis et al., 2017; Rades et al., 2018; Sohbati et al., 2012a, 2015; Souza et al., 2019, 2021); hence, the signal must have been bleached at one time. The time of burial of rock surfaces is calculated by dividing the measured palaeodose with depth-dependent dose rates (e.g., Gliganic et al., 2021; Greilich et al., 2005; Liritzis, 2001; Liritzis et al., 2010; Rades et al., 2018; Sohbati et al., 2015; Souza et al., 2019), or, more experimentally, by fitting the signal-depth profiles from buried or covered rock surfaces (Freiesleben et al., 2015; Sohbati et al., 2015).

The advantage of burial dating dry-stone walls using rock surface luminescence dating is that if the rock surface was sufficiently exposed before being covered during construction, this surface should directly record the construction time, provided that no subsequent rearrangement at the structure further reset the signal. If rearrangement occurred, then it is conceivable that complex life histories of sites can be reconstructed using rock surface luminescence dating since multiple burial and exposure events can be recorded in the luminescence-depth profiles (Freiesleben et al., 2015; Rades et al., 2018). Previous attempts of burial dating of stone structures using the rock surface luminescence technique have been encouraging when applied to various lithologies, time spans, and archaeological settings (e.g., Galli et al., 2020; Greilich et al., 2005; Liritzis and Vafiadou, 2015; Liritzis et al., 2019b; al Khasawneh et al., 2019a,b). An application of exposure dating using rock surface luminescence has been the temporal constraining of rock art by dating adjacent rock falls (Chapot et al., 2012; Sohbati et al., 2012b; Liritzis et al., 2019a). Exposure dating of dry-stone structures using rock surface luminescence dating could provide minimum ages for the
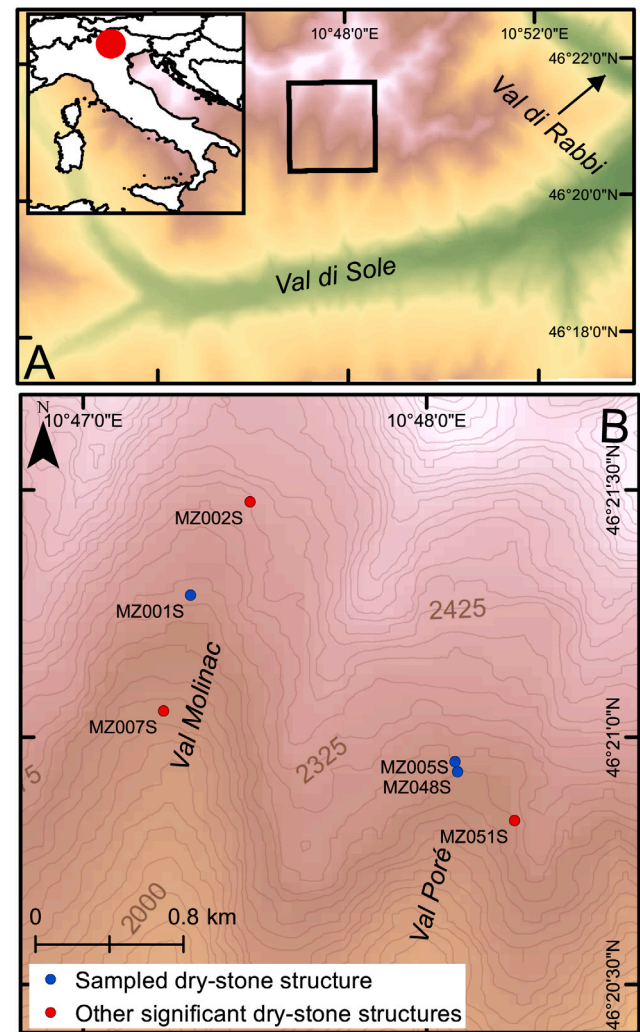

Fig. 1. Map of Val di Sole (A), where the black square outlines the study area in Val Molinac and Val Poré (B).

construction of such structures. The system is sensitive to millimetre-scale changes in luminescence-depth profiles and is suitable for dating decades to centuries-old dry-stone structures.

The specific objective of this study is to investigate the possibilities of using rock surface luminescence dating of stone structures to constrain the construction of three partly preserved dry-stone walls belonging to structures previously dated with radiocarbon and archaeological assemblages to the Middle Ages–Modern Period. We present novel chronological data collected from dry-stone structures. We investigate bleaching depths and burial and exposure ages of rock surfaces from intact and degraded walls by measuring the luminescence emission from feldspar grains from polymineral rock slices. The results are discussed regarding the chronological context of specific structures, including the interpretation of age scatter from presumably isochronous surfaces, along with general considerations for dating dry-stone structures.

2. Study site

2.1. Site context

The selected sites are located in Val Molinac and Val Poré (Fig. 1), south-facing, tributary valleys to the tectonic valley Val di Sole, located in the central-eastern Italian Alps. The valley is permanently settled up to ∼1500 m above sea level, with only seasonal dwellings located at

higher altitudes. The geology is dominated by metamorphic, gneissic (mostly paragneisses with some orthogneisses) rocks from the Ulten unit (Dal Piaz et al., 2007). The environment in the upper parts of these tributary valleys predominantly shows glacial and periglacial features, with meadows covering the valley ends. While the current climatic conditions are insufficient to sustain glaciers, the valley heads of both Val Poré and Val Molinac had been shaped by cirque glaciers during the Pleistocene. Other prominent features are inactive rock glaciers, talus formations, gravitational slope deformation and other hillslope and gelifluction features (Angelucci et al., 2014).

2.2. Dry-stone structures in Val Poré and Val Molinac

The landscape in Val Poré and Val Molinac shows clear signs of long-term anthropogenic impact. Over eighty dry-stone structures (all located in an alpine environment above 2000 metres of elevation) have been identified during surveys by the project *Alpine Landscapes: Pastoralism and Environment of Val di Sole* (ALPES) (Angelucci and Carrer, 2015; Angelucci et al., 2017, 2021; Carrer and Angelucci, 2013, 2018). The structures mentioned in this work are marked in Fig. 1B. Stone structures are recorded at high altitudes in the Alps date from the late Neolithic and early Bronze Age to the modern period (e.g., Reitmaier et al., 2013; Walsh et al., 2014). In Val Poré and Val Molinac, such structures vary in size and character and have been subdivided by Carrer and Angelucci (2013) into three categories: enclosures, huts, and rock shelters. Most enclosures are compound structures consisting of several enclosures and a hut. The primary construction technique placed elongated gneissic boulders perpendicularly to the wall direction. Additional archaeological finds are scarce from the surveyed structures (Angelucci et al., 2014), but excavations from enclosures MZ005S and MZ051S in Val Porè have documented archaeological artefacts and provided insights into their occupation history (Angelucci et al., 2021; Carrer and Angelucci, 2013; Dell'Amore et al., 2017; Medici et al., 2014). Archaeological investigations revealed that, although evidence of human occupation in the area dates back to the Early Bronze Age (Angelucci et al., 2021), pastoral activities intensified from the late Middle Ages and the early modern period (Carrer and Angelucci, 2018). Our dating efforts here focus on three dry-stone structures (Fig. 2): two enclosure complexes (MZ001S and MZ005S) and a hut (MZ048S).

2.2.1. MZ001S — enclosure complex
MZ001S (Fig. 2A) is the largest structure so far discovered in the upland areas of Val di Sole. This site consists of three enclosures and a hut, located at 2293 m.a.s.l. in Val Molinac. The dry-stone walls are generally well-preserved, and the site's characteristics suggest its possible early Modern age. No excavations have so far been conducted at MZ001S, but a 19th century AD potsherd was discovered inside the hut during a survey of the structure (Dell'Amore et al., 2017).

2.2.2. MZ005S — enclosure complex
The enclosure complex MZ005S (Fig. 2B) was constructed in the Val Porè at 2257 m.a.s.l. The first results from excavations and structural analyses suggest that MZ005S consists of one hut and three enclosures, constructed and restored in five different phases (Carrer and Angelucci, 2013). The most recent enclosures are still well-defined, with mostly intact walls. The dry-stone walls forming the third, smaller and older enclosure have partly collapsed. Excavations in two test pits (one pit in the northernmost enclosure and one in the oldest enclosure) have unearthed two archaeological layers belonging to the current, and a buried A horizon. The artefact assemblage recovered from MZ005S consists of iron nails and rivets, an iron key, a coin and a glass bead, attributed to the Late Medieval and Early Modern period (Carrer and Angelucci, 2013; Medici et al., 2014). In particular, the coin and the glass bead were produced in Venice (Italy) in the mid-16th century AD. Additional flint and potsherd finds indicate an earlier occupation
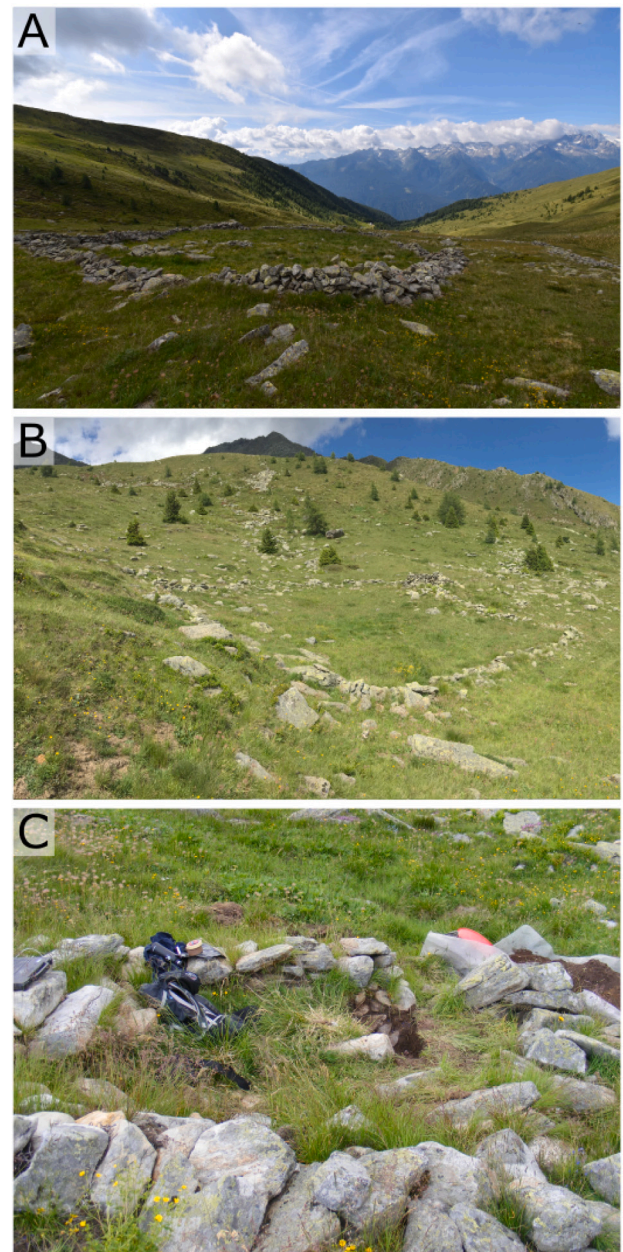
Fig. 2. The sampled dry-stone structures in Val Molinac (MZ001S; A) and Val Poré (MZ005S; B, MZ048S; C).

during prehistoric times. Charcoal fragments from the excavation gave radiocarbon ages of 1405–1438 cal AD, 1519–1645 cal AD, and the 20th century, while a charcoal fragment from a test-pit in the northern enclosure resulted in an age of 652–776 cal AD (Angelucci and Carrer, 2015; Carrer and Angelucci, 2013).

2.2.3. MZ048S — hut
The dry-stone structure MZ048S (Fig. 2C) is a hut located a few metres south of MZ005S. The structure appears affected by gravitational movement of the slope, and a section of a partly intact wall is buried. Only a single flint fragment was recovered from beneath the base of MZ048S, and its association with the hut is currently not fully understood (Dell'Amore et al., 2017). The radiocarbon age of 677–878 AD was obtained from a charcoal fragment collected inside the structure (Angelucci and Carrer, 2015). Two additional charcoal samples from silty sediments beneath the structure provided radiocarbon

Table 1
List of collected samples from Val Molinac and Val Poré.

Lab. ID	Sample name	Structure/location	Sample type	Field context
C-L4632	MZ048S-1	MZ048S	Buried rock	Part of hut wall
C-L4633	MZ048S-2	MZ048S	Buried rock	Part of hut wall
C-L4634	MZ005S-1	MZ005S	Buried rock	Partly buried in degraded wall of the oldest enclosure
C-L4635	MZ005S-2	MZ005S	Buried rock	Wedged between larger rocks in the degraded wall of the oldest enclosure
C-L4637	MZ001S-1	MZ001S	Exposed rock	Wedged sample from intact part of wall, surface facing W.
C-L4638	MZ001S-2	MZ001S	Exposed rock	Wedged sample from intact part of wall, surface facing W.
C-L4962	MZ005S-CAL	Boulder near MZ005S	Calibration surface	Exposed for one year, surface facing E.
C-L4963	MZ001S-CAL-1	Boulder near MZ001S	Calibration surface	Exposed for one year, surface facing N.
C-L4965	MZ051S-CAL	Bedrock outcrop near MZ051S	Calibration surface	Exposed for one year, surface facing E.
C-L4966	MZ001S-3	MZ001S	Exposed rock	Positioned on top of partly collapsed complex wall, surface facing S.

ages from the early 5th millennium BC (Angelucci and Carrer, 2015), possibly dating mid-Holocene forest wildfires in Val Poré.

3. Materials and method

3.1. Sampling, preparation, and luminescence measurements

Gneissic rocks were collected from the dry-stone structures during excavation campaigns in the summers of 2018 and 2019 (supplementary material: Fig. A.1 and A.2). The samples (Table 1; for photographs, see also supplementary material: Fig.A.3) were immediately covered in opaque plastic bags to protect the surfaces from exposure to daylight. The exposed surfaces (all from enclosure complex MZ001S) were marked on the samples at the time of collection. Samples MZ001S-1 and MZ001S-2 were wedged between other rocks, while sample MZ001S-3 was sampled from the top of the enclosure wall. The calibration surfaces were exposed by removing the outer part (∽3 cm for sample MZ001S-CAL-1; more for other samples) of boulders and outcrops in 2018. They were subsequently collected after one year of exposure in 2019.

The top and bottom surfaces of the buried rocks were marked during sampling. The rocks from MZ048S had been placed into the wall stacked on top of each other during construction. MZ005S-1 was partly buried as part of the degraded enclosure wall from the oldest enclosure at MZ005S.MZ005S-2 was collected from the same wall but was positioned with its longest axis perpendicular to the ground in contrast to the other buried rocks. Hence, the terms "top" and "bottom" are, strictly speaking, arbitrary for MZ005S-2 and are used only to differentiate between the two surfaces.

The rocks were prepared for measurement following Sohbati et al. (2011): cores were extracted with a bench drill and sliced into ∽0.7 mm thin slices. Areas of the rock surfaces that might have been exposed to light before sampling were carefully avoided during coring.

All samples were measured in a RisøTL/OSL reader (model DA-20) (Bøtter-Jensen et al., 2010) in the Cologne Luminescence Laboratory, using intact slices mounted directly in the sample carousel. We used only infrared stimulated luminescence (IRSL) of feldspars since no separation between quartz and feldspars is possible during the preparation of intact slices. The sensitivity-corrected luminescence (L_n/T_n) with depth was measured in the exposed samples using a IRSL protocol (e.g., Sohbati et al., 2011) (50 °C stimulation for 300 s). For the buried samples, a post-infrared IRSL (pIRIR) protocol (e.g., Thomsen et al., 2008) (first IRSL, then pIRIR at 130 °C for 300 s) was applied to all slices. The equivalent doses (D_e) in the outer slices were measured using cycles of increased regenerative dosing (see Murray and Wintle, 2000). Since the feldspar signal in IRSL and low-temperature pIRIR protocols are known to be subjected to anomalous fading, correcting for this signal loss is common practice when calculating burial ages (e.g., Brill and Cisternas, 2020; Reimann et al., 2011). We corrected for fading using the approach of Huntley and Lamothe (2001). The reproducibility of the measurement protocol used to date the buried samples was assessed with a dose recovery test (Fig. 3). The initial IRSL signal provides acceptable dose recovery for all samples following 2.6–6.0 Gy
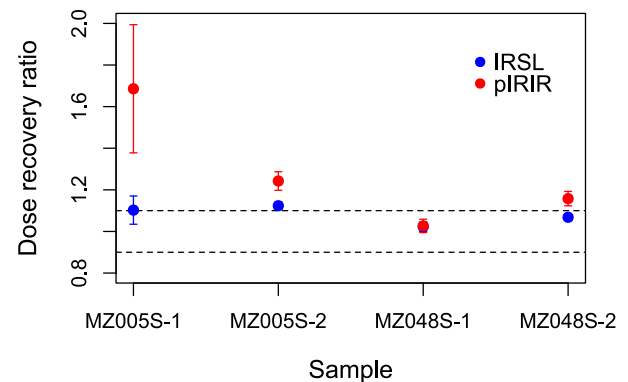

Fig. 3. Dose recovery ratios for IRSL and pIRIR signals from the buried rocks.

of beta radiation, while the pIRIR signal tends to overestimate the given dose. Therefore, we only proceeded with analysis by using the IRSL signal. Further details regarding the measurement protocols, fading corrections, and example dose–response curves (Fig B.5) are presented in the supplementary material.

3.2. Dose rate

Knowledge about the rate of environmental irradiation to the feldspar grains in the rocks is required to calculate burial ages from the rock surfaces. The dose rate depends on the radionuclide concentration in the rocks themselves and the surrounding sediments, the internal potassium content and the size of the feldspar grains, and the amount of cosmic radiation which reaches the rocks. We used high-resolution gamma spectrometry (Murray et al., 1987) to measure the concentrations of naturally occurring radionuclides in the sampled rocks from MZ005S and MZ048S (Table 2). The radionuclide content from the surrounding material was assumed to be the average of the four rocks sampled from MZ005S and MZ048S and the four rocks from the same geological unit (collected from archaeological layers in structure MZ051S) dated by Ageby et al. (2021). We converted the radionuclide concentrations into beta and gamma dose rate components using the conversion factors of Cresswell et al. (2018) and assumed that the moisture content in the rocks was insignificant. Infinite-matrix dose rates were calculated using *R* v. 4.1.1 (Team, 2021) with the *calc_CobbleDoseRate()* package (Riedesel and Autzen, 2021) from the *Luminescence* package (Kreutzer et al., 2021), which uses attenuation factors for beta and gamma radiation from Riedesel and Autzen (2020) to calculate depth-dependent dose rates. The internal potassium concentration in feldspar grains from Val di Sole gneisses was measured with *μ*-XRF by Ageby et al. (2021). We here estimated the internal potassium contribution from the feldspar in our rocks by using an average concentration from the data reported by Ageby et al. (2021). For internal potassium, the average feldspar grain size was assumed to be 400 μm, based on visual inspections of thin sections of previously collected rocks from the same geological units in Val di Sole. Cosmic dose rate was calculated following Prescott and Hutton (1994).

Table 2

Summary of radionuclide concentrations and attenuated dose rates in the buried rocks and the average from eight gneissic rocks from Val Poré.

Sample	Radionuclide concentration				Dose rate (Gy ka⁻¹)			
	^{238}U (ppm)	^{232}Th (ppm)	^{40}K (%)	Internal K (%)	Gamma	Beta	Cosmic	Internal K
MZ048S-1	2.04 ± 0.11	7.67 ± 0.46	3.31 ± 0.04	1.00 ± 0.28	1.42 ± 0.02	2.80 ± 0.22	0.29 ± 0.03	0.13 ± 0.07
MZ048S-2	2.63 ± 0.14	14.34 ± 0.84	0.70 ± 0.01	1.00 ± 0.28	1.17 ± 0.02	1.10 ± 0.07	0.29 ± 0.03	0.13 ± 0.07
MZ005S-1	2.40 ± 0.13	8.04 ± 0.48	1.58 ± 0.02	1.00 ± 0.28	1.05 ± 0.02	1.58 ± 0.11	0.38 ± 0.04	0.13 ± 0.07
MZ005S-2	3.10 ± 0.16	15.40 ± 0.89	1.48 ± 0.02	1.00 ± 0.28	1.47 ± 0.03	1.74 ± 0.11	0.38 ± 0.04	0.13 ± 0.07
Average rock	2.25 ± 0.25	9.62 ± 1.47	1.43 ± 0.24					

3.3. Fitting of luminescence-depth profiles and exposure ages

Average luminescence-depth profiles (calculated from two or more cores from each surface) were fitted with *R* v. 4.1.1 (Team, 2021), using the *nls()* function. The calibration and exposed surfaces were fitted using the equation:

$$L = L_0 e^{-t_e \overline{\sigma\varphi_0} e^{-\mu x}} \tag{1}$$

following the model proposed by Sohbati et al. (2011), where L is the luminescence intensity (i.e., L_n/T_n) measured in a specific slice, L_0 is the saturated luminescence intensity, t_e is the exposure time, $\overline{\sigma\varphi_0}$ is the bleaching rate at the rock surface based on the photoionising cross-section (σ) and the photon flux (φ_0), μ is the attenuation of light penetration with depth (x). Following the approach first used by Sohbati et al. (2012b), we constrained $\overline{\sigma\varphi_0}$ by using the calibration surfaces with a known t_e, before calculating the t_e for the exposed surfaces. The buried surfaces were fitted following the model developed by Freiesleben et al. (2015), which allows for fitting of an exposure followed by a burial events:

$$L = (L_0 e^{-t_e \overline{\sigma\varphi_0} e^{-\mu x}} - 1)e^{-F(x)t_b} + 1 \tag{2}$$

where $F(x)$ is the ratio between depth-dependent dose rate and the characteristic dose (D_0) and t_b is the burial age. Additional exposure and burial events can be added to fit the shape of the luminescence-depth profiles (Freiesleben et al., 2015). All L_n/T_n values were normalised by the arithmetic mean L_n/T_n derived from saturated slices. All buried surfaces were fitted with a final burial event since these rocks were buried at the time of sampling. The pre-burial luminescence depth profiles were subsequently modelled (e.g., al Khasawneh et al., 2019a) using $t_e \overline{\sigma\phi_0}$ and μ from the fit to assess depth of complete bleaching ($L < 0.001$) before burial. The exposed rock surfaces were fitting using no weighting; the covered surfaces were fitted by weighting the profiles by the standard error; both using the *nls()* function.

4. Results

4.1. Calibration surfaces and exposed rock surfaces from MZ001S

A summary of the results from the exposure dating from structure MZ001S is presented in Table 3. Luminescence-depth profiles are presented from calibration and exposed surfaces from Val Molinac and Val Porè (Fig. 4). The depth of the bleaching front (<50% of field saturation) for the IRSL signal varies considerably between the different surfaces. This variation is especially notable for the exposed surfaces of unknown exposure ages (MZ001S-1–MZ001S-3), in which the depth of the bleaching front varies between 1.1 to 11.2 mm. The depth variation is lesser in the calibration surfaces, ranging between 1.5 to 3.2 mm. The site-specific bleaching rate ($\overline{\sigma\phi_0}$) at the rock surfaces for Val Molinac and Val Poré is fitted to be 29.59 ± 16.10 a⁻¹ based on three calibration surfaces. The fitted exposure ages (t_e) from structure MZ001S using $\overline{\sigma\phi_0}$ ranges between 0.1 a (i.e., younger than the calibration surfaces) for MZ001S-2, to 93 ± 58 a for MZ001S-3.

Table 3

The results from fitting (Eq. (1)) of the calibration and exposed surfaces from Val Porè and Val Molinac. A $\overline{\sigma\phi_0}$ of 29 a⁻¹ was used to calculate the exposure ages (t_e) for the exposed surfaces.

Sample	μ mm⁻¹	Bleaching depth (mm) 50% of field saturation	t_e (a)
MZ001S-CAL-1	1.18 ± 0.17	3.2	1
MZ005S-CAL	2.59 ± 0.38	1.5	1
MZ051S-CAL	1.38 ± 0.21	2.7	1
MZ001S-1	1.08 ± 0.12	5.5	15 ± 8
MZ001S-2	1.26 ± 0.36	1.1	0.1 ± 0.02
MZ001S-3	0.72 ± 0.04	11.2	93 ± 58

4.2. Burial dating of MZ048S and MZ005S

The luminescence-depth profiles (Fig. 5) show that L_n/T_n is significantly lower at the rock surfaces compared to saturated plateaus observed deeper into the rocks. The IRSL intensity has reached saturation at ⌣4 mm in all samples except MZ048S-1, in which saturation is reached at ⌣11 mm. All surfaces have at the minimum two slices with a L_n/T_n (normalised for field saturation) <0.2 except for the top surface of MZ005S-1. The parameters used for fitted profiles in Fig. 5 are reported in Table 4. The fitted profiles indicate that all surfaces, except the top surface of MZ005S-1, have experienced at least one burial event; MZ048S-1 is fitted for three burial events. The modelled pre-burial luminescence-depth profiles (for MZ048S-1; this is the profile before the final burial as part of the wall of MZ048S) indicate that the IRSL signal in the surface slices in all of the profiles was bleached before the last burial (see dotted line in Fig. 5). For structure MZ048S, the most recent fitted burial ages are estimated to be 1.9 ± 0.3 ka (MZ048S-1) and 4.1 ± 0.1 ka (MZ048S-2). The two previous burial events observed in MZ048S-1 are estimated to have occurred at 8.1 ± 1.1 ka and 19.0 ± 5.7 ka, respectively. The fitted burial ages (t_b) from the rocks from MZ005S, which varies considerably between the different surfaces, are estimated to be: 0 a (MZ005S-1; top surface), 0.7 ± 0.3 ka (MZ005S-1; bottom surface), 1.2 ± 0.1 ka (MZ005S-2; top surface), and 9.0 ± 3.2 ka (MZ005S-2; bottom surface).

The ages derived from D_e measurements are presented in Table 5. The calculated mean burial age from the surface slice from MZ048S-1 is 1010 ± 170 a, yielding a fading corrected age of 1030 ± 180 a. The surface slice of MZ048S-2 is dated to 1450 ± 100 a (uncorrected age is 1200 ± 60 a). For MZ005S-1, the surface slice from the top surface yields a recent mean age of 180 ± 50 a, fading corrected to 220 ± 60 a. The surface slice for the bottom is estimated to be of similar age at 160 ± 70 a (the uncorrected age is 130 ± 60 a). The surface slice from the top surface MZ005S-2 is dated to 3750 ± 660 a, while the bottom surface is younger at 500 ± 60 a (both ages are fading-corrected).

5. Discussion

5.1. Context for the luminescence ages

This study has measured the luminescence ages of three distinct dry-stone structures: MZ048S, MZ005, and MZ001S. All fitting of luminescence-depth profiles in this study (Figs. 4–5) was attempted using a double exponential approach (e.g., Freiesleben et al., 2015;
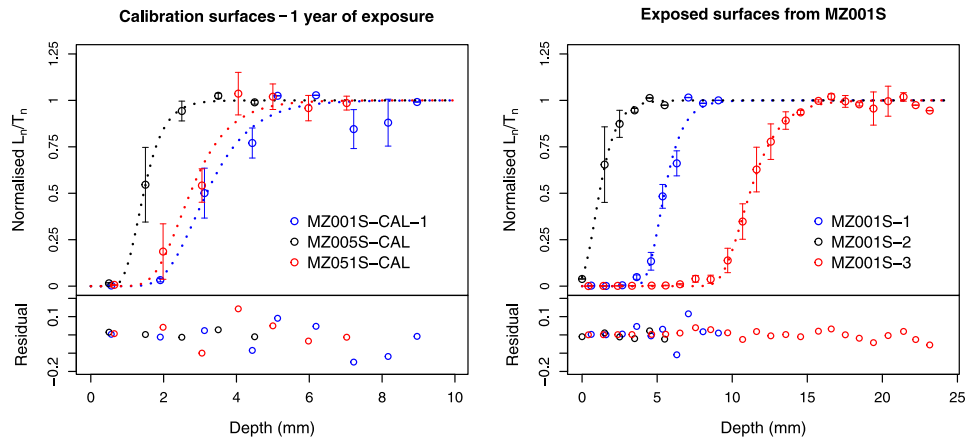
Fig. 4. Fitted luminescence-depth profiles for calibration surfaces exposed in Val di Sole for one year (left) and exposed surfaces from MZ001S-1 (right), fitted (dotted line) using the model $L(x) = L_0 e^{-t_e \overline{\sigma \phi_0} e^{-\mu x}}$ (Sohbati et al., 2011). The exposed surfaces were fitted using $\overline{\sigma \phi_0}$ derived from the calibration surfaces.
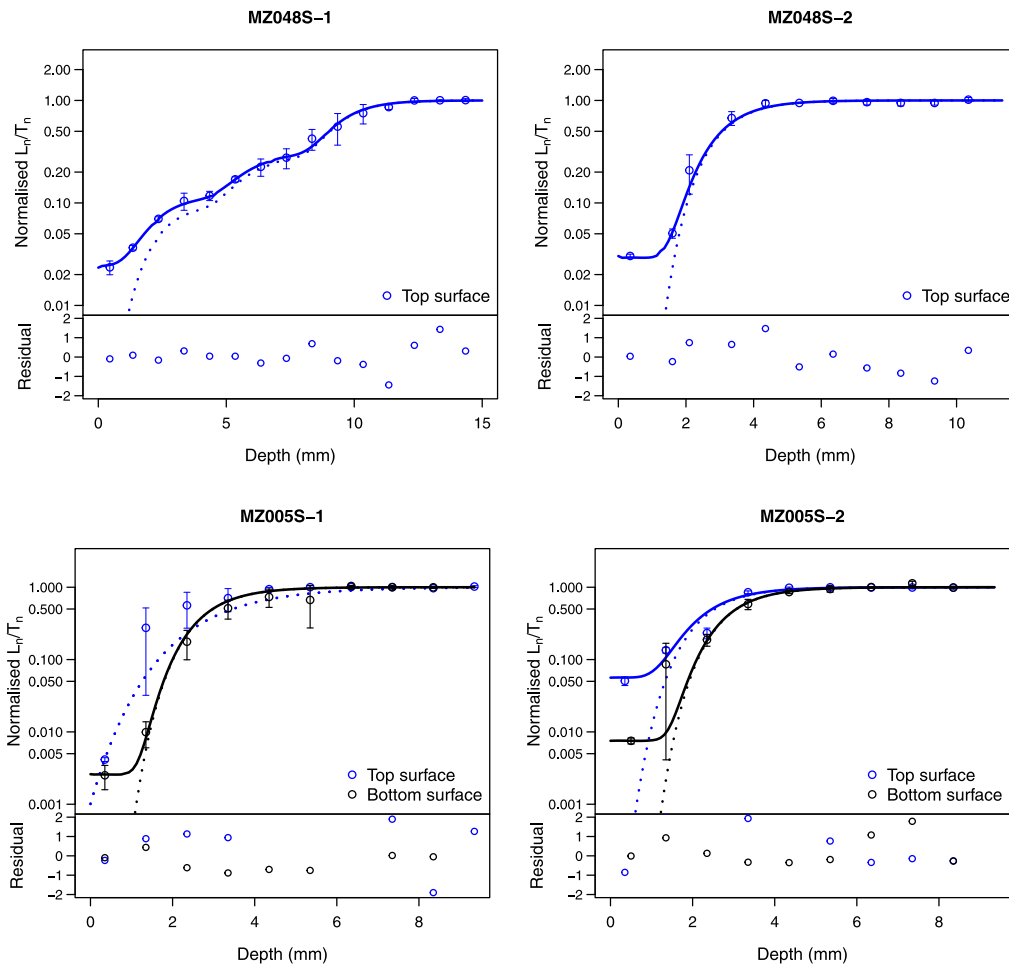

Fig. 5. Luminescence-depth profiles with 1σ error bars from dry-stone structures MZ005S and MZ048S. Best-fit burial profiles (solid lines) are plotted with corresponding fitting residuals. Modelled exposure profiles (dotted lines) are plotted as well; these profiles represent the exposure event before the final burial, reset to 0.1% of the saturated signal between ~0–2 mm depending on surface and sample. The fitted and modelled profiles are identical for the top surface of MZ005S-1 ($t_b = 0$); hence no solid line is plotted. No fitting is attempted for the bottom surfaces of MZ048S-1 and MZ048S-2 due to the unsuitable luminescence-depth profiles. Normalised L_n/T_n values are plotted on a logarithmic scale.

Sohbati et al., 2011). An alternative approach to fitting signal-depth profiles was proposed by (Laskaris and Liritzis, 2011); they instead suggested using cumulative log-normal fitting, demonstrating the relationship of the observed luminescence to the exposure time and the depth below the rock surface. Comparisons between simulated

signal-depth profiles have indicated a similarly good fit using either approach (Liritzis et al., 2017).

The spatial relationship between MZ048S-1 and MZ048S-2 (placed on top of each other) determines that they were likely positioned as part of the wall simultaneously; hence, the top surfaces of both rocks

Table 4
Parameters used for fitting (Eq. (2)) luminescence-depth profiles in Fig. 5. D_0 is assumed to be identical for both top and bottom surfaces.

Sample	Surface	Burial events	D_0 (Gy)	μ mm^{-1}	$t_e \overline{\sigma \phi_0}$	$t_{e2} \overline{\sigma \phi_0}$	$t_{e3} \overline{\sigma \phi_0}$	t_b (a)	t_{b2} (a)	t_{b3} (a)
MZ005S-1	Top	0	818 ± 29	0.66 ± 0.13	7 ± 2			0		
MZ005S-1	Bottom	1		1.23 ± 0.22	27 ± 11			706 ± 315		
MZ005S-2	Top	1	508 ± 21	1.20 ± 0.20	15 ± 7			9027 ± 3188		
MZ005S-2	Bottom	1		1.26 ± 0.15	34 ± 13			1179 ± 108		
MZ048S-1	Top	3	334 ± 10	1.03 ± 0.13	8 ± 12	309 ± 483	13062 ± 6975	1923 ± 277	8124 ± 1133	18972 ± 5732
MZ048S-2	Top	1	348 ± 6	1.13 ± 0.04	23 ± 2			4062 ± 146		

Table 5
Results from the buried rocks from structures MZ005S and MZ048S. Sample-dependent g-values (normalised for 2 days), depth-dependent slice dose rates, D_e, and uncorrected and fading-corrected IRSL ages.

Sample	Surface	g-value $_{2days}$ (%/decade)	Slice depth (mm)	Slice dose rate (Gy ka^{-1})	Mean D_e (Gy)	n	Uncorr. age (ka)	Corr. age (ka)
MZ048S-1	Top	0.25 ± 0.54	0.0–0.7	4.16 ± 0.33	4.18 ± 0.70	4	1.01 ± 0.17	1.03 ± 0.18
MZ048S-2	Top	2.20 ± 0.49	0.0–0.7	2.64 ± 0.26	3.17 ± 0.13	2	1.20 ± 0.06	1.45 ± 0.10
MZ005S-1	Top	2.46 ± 0.69	0.0–0.7	3.02 ± 0.29	0.55 ± 0.11	4	0.18 ± 0.05	0.22 ± 0.06[a]
MZ005S-1	Bottom	2.46 ± 0.69	0.0–0.7	3.02 ± 0.29	0.40 ± 0.17	3	0.13 ± 0.06	0.16 ± 0.07
MZ005S-2	Top	2.34 ± 0.50	0.0–0.7	3.27 ± 0.31	10.08 ± 1.67	3	3.08 ± 0.51	3.75 ± 0.66
MZ005S-2	Bottom	2.34 ± 0.50	0.0–0.7	3.27 ± 0.31	1.38 ± 0.15	2	0.42 ± 0.05	0.50 ± 0.06

[a] Upper limit age estimate.

should yield the same ages for their last burial event. Despite this expectation, the ages derived from the fitting show that t_b of MZ048S-1 (∽1900 a) is ∽50% younger as compared to MZ048S-2 (∽4100 a). This suggests that our fitted ages are unreliable; a sentiment previously expressed by al Khasawneh et al. (2019a), who pointed out that fitted ages are less reliable due to the assumption of common D_0. Instead, we favour the ages calculated from average D_e values for dating the most recent burial event (t_b). Since our main objective in this study is to investigate the application of rock surface dating to dry-stone structures, we did not measure individual D_e for the older burial events from MZ048S-1 since these events predate human occupation of the upland areas of Val di Sole as is currently understood (e.g., Angelucci et al., 2021). Instead, these ages seem to constrain geomorphological events occurring during the Late Pleistocene and the Holocene as part of the landscape evolution in Val Poré.

The original context of the burial events recorded in the luminescence-depth profile from MZ048S-1 is unknown since the rock was likely moved during exposure by natural processes or by humans. Accordingly, based on the fitted ages, we can only speculate on the processes that caused the exposure and burial events observed in the luminescence-depth profile. The oldest burial event (t_{b3} ∽13-25 ka) is likely connected to glacial oscillation following the last glacial maximum, which would roughly fit with the timing of deglaciation in the adjacent (Favilli et al., 2009). The oldest known soil formation in Val Molinac and Val Poré was dated to the 7th millennium BC by Angelucci and Carrer (2015) and the second burial event (t_{b2}) is dated to this period. Thus, following the re-exposure of MZ048S-1, the rock was re-buried, perhaps by slope or periglacial processes. Finally, the rock was exhumed before being buried a third and last time as part of the wall of MZ048S; it is this event (t_b) we can date by measuring the palaeodose from slices. Since the fitting of MZ048S-1 indicates that the pre-last burial bleaching front reaches approximately the depth of the second slice at 2 mm depth (Fig. 5; dotted line), it is conceivable that the second slice of MZ048S-1 does record the correct burial age, with little pre-burial residual dose. If so, the burial age of the surface slice underestimates the burial age, perhaps due to bleaching during sampling, poorly constrained external beta dose rate at surface/surrounding material interface, light penetrating through gaps, or the top surface of MZ048S-1 was briefly re-exposed (even if the rock was never moved) at ∽1000 AD during an otherwise undated restoration phase MZ048S-1.

The shape of the luminescence-depth profiles from MZ005S-1 and MZ005S-2 are mostly like MZ048S-2, i.e., a single burial event is represented by a short burial plateau (t_b; Fig. 5; solid lines), succeeding

the pre-burial exposure events (Fig. 5; dotted lines). This is not the case at the top surface of MZ005S-1, where the signal-depth profile displays ambiguity in the fitting dependent on whether the signal was sufficiently bleached before burial. This, we cannot assess since the fitted profile shows no significant bleaching front. Further fitting uncertainty arises due to inter-core variations in the shape of the luminescence-depth profile, as is shown by the significant standard errors at depths ∽1-4 mm. A significant error in luminescence is also observable to a lesser degree at the bottom surfaces of MZ005S-1 and MZ005S-2. Inter-core variations between luminescence-depth profiles from cores extracted from the same rock surface have been described by Meyer et al. (2018), who attributed it to spatial variation in the mineralogy when dark minerals could inhibit light from penetrating deeper into some areas of the rock surfaces. Such variations cause significant ambiguity in the fit, which must be adjusted by weighting for the luminescence error during fitting. A likely but untested explanation for some luminescence-depth variations in our samples since e.g., biotites are common in the Val di Sole gneisses (Ageby et al., 2021; Dal Piaz et al., 2007) see also supplementary material Fig A.4. Despite the uncertainty in the fitting (especially for the top surface of MZ005S-1 and the bottom surface of MZ005S-2), we can still calculate ages from D_e to estimate the upper age limit for when the surfaces were covered.

The ages from the top and bottom surfaces of MZ005S-1 agree at 1σ (1740–1860 AD and 1790–1930 AD for top and bottom surfaces, respectively) but are at least 180 years younger compared to the age derived from the bottom surface from MZ005S-2 (1460–1580 AD). While these ages are all chronologically consistent with the occupation at MZ005S from the Late Middle Ages until the mid-20th century (Carrer and Angelucci, 2013, 2018), the age difference between MZ005S-1 and MZ005S-2 could perhaps be explained by the recent history of the samples. Possibly, MZ005S-2 was not turned during the degradation of the wall; this would be consistent with how an older event (2400–1100 BC) remains recorded at the top surface. On the other hand, MZ005S-1 must have been turned recently since the surface slices at both surfaces have a small (∽0.5 Gy) palaeodose. Possibly, the wedged position of MZ005S-2 in the wall protected the degradation of the wall; hence, the top surface could represent a repair of the wall during a time of intense occupation during the Late Medieval period and the Early Modern period, as demonstrated by the archaeological assemblage which strongly points to significant human activity at this time (Angelucci et al., 2014; Carrer and Angelucci, 2013; Medici et al., 2014). The burial event from the bottom surface of MZ005S-2 generally concurs with the dating of the buried enclosure MZ051S, where Angelucci et al. (2021) has identified human activity in the Early Bronze Age. The potsherds

recovered from MZ005S (Carrer and Angelucci, 2013) indicate human presence at the site during the Late Bronze Age to the Early Iron Age, which here appears to agree with rock-surface luminescence dating. Accordingly, we must now consider the possibility that the construction of MZ005S started at some point during the Bronze Age, just like at the nearby MZ051S.

Constraining the archaeological chronology of MZ001S to the 19th century AD is solely based on a single potsherd (Dell'Amore et al., 2017). Despite the weak age control, the young ages derived from the fitting of MZ001S-1 and MZ001S-2 are clearly too recent and do not contain any valid chronological information regarding the construction or use of MZ001S. The age from MZ001S-3 would fit the preliminary assessment that MZ001S was constructed at the latest in the 19th century. However, at this time, without a systematic sampling of all areas of the enclosure, we cannot determine if the age of MZ001S-3 represents the initial construction of MZ001S or a later building or repair phase occurring in the late 19th or early 20th century.

5.2. Rock surface luminescence dating of dry-stone walls

A plausible explanation for the age underestimation of MZ001S-1 and MZ001S-2 and short luminescence-depth profiles is that the luminescence-depth profiles were shortened by erosion. Since weathering and subsequent erosion of surface grains will shorten the bleaching profiles, the model (Eq. (1)) only estimates the minimum exposure age (Sohbati et al., 2012b). Post-glacial erosion rates at the Mount Blanc massif varied on scales between 10^{-3} and 10^{0} mm a^{-1} at different natural rock surfaces (Lehmann et al., 2019b). While erosion rates of rock surfaces are beyond the scope of this study, such erosion rates, unless corrected for, will lead to severe age underestimations considering that Lehmann et al. (2019a) showed how steady-state erosion rates at 10^{-4} mm a^{-1} or higher would affect the luminescence-depth profiles. Friction due to rubbing between stone blocks of covered surfaces has also been proposed to cause shortening of luminescence-depth profiles (Liritzis et al., 2015, 2016). Considering how sensitive exposure dating is to erosion (Lehmann et al., 2019a), it appears reasonable that using such an approach to date dry-stone structures is only feasible in specific settings where erosion of exposed rock surfaces is limited. At the same time, good knowledge of geological context, geomorphological evolution, and past human impact is paramount for interpreting dating results. The new chronological data from MZ048S show that it is possible to provide direct ages from dry-stone walls with few associated archaeological artefacts using rock surface luminescence dating of buried surfaces. With rock surface luminescence dating, any structure with a sufficiently translucent lithology containing feldspars or quartz could be targeted. The possibility of providing such data is exciting since many dry-stone walls currently lack numerical dating of their construction. The scattered ages from MZ005S demonstrate that understanding the context of samples is necessary to interpret the ages. It appears that rocks collected from degraded walls could have disturbed luminescence-depth profiles concerning the initial construction of the wall. In the ideal case, such events could be preserved in luminescence depth profiles (as shown by the complex profile of MZ048S-1); then, ages could be derived for both the construction and the degradation of the wall. This is not the case for our MZ005S samples, for which all the luminescence-depth profiles showed a maximum of one exposure and burial event. Considering that erosion appears to be an issue at our alpine site, deep luminescence-depth profiles might be rare due to the shortening of the profiles as grains have been removed. Also, since lithology is essential for how deep the bleaching fronts reach during a given period, as was shown by bleaching experiments by Ou et al. (2018), other lithologies might more often show deeper bleaching fronts; this is usually preferable since each dose plateau becomes more distinct compared to plateaus from less translucent rocks. The luminescence-depth profiles in translucent samples, however, are likely more sensitive to bleaching if light can penetrate between the stones

when placed in the wall. Overall, it should be noted that the buried surfaces we sampled in Val Poré showed significant variations in the depth of the bleaching front, and for MZ005S-1 and MZ005S-2, variations in ages. Considering the quite degraded state of the sampled wall and the clear signs of multiple phases of construction at MZ005S (Carrer and Angelucci, 2013), variations between ages from different surfaces might be unavoidable for such a structure, and the variation might provide valuable information anyway. Scatter between ages is not always observed since previous dating attempts of stone structures using rock surface luminescence dating by al Khasawneh et al. (2019b) produced indistinguishable ages at ⌣10 ka, derived from a rock slab and two rocks. Future dating efforts of the Val Poré (and Val Molinac) dry-stone structures should include more surfaces to corroborate the ages presented here since increasing the number of samples should help more definitely resolve the history of the dry-stone enclosure complex MZ005S.

6. Conclusions

Using IRSL dating, our work from two dry-stone structures from Val Poré has provided new chronological data regarding the construction and life history of huts and enclosures used for purposes of pastoralism. Thus, we show that rock surface luminescence burial dating is a practical, albeit not a completely straightforward, tool for dating such structures. The depth of resetting varies between the different surfaces, meaning that in some cases, it is advisable to sample several specimens in case some surfaces were insufficiently bleached before the rocks were placed in the walls. The two rocks from MZ048S were collected from a mostly intact wall where the rocks likely remained in position since construction. These top surfaces show a similar final burial age, indicating that we can constrain the construction of this wall to the Early Middle Ages. One of these rocks also displayed a complex history of two older burial events. In our case, these events are associated with the landscape evolution in the uplands of Val di Sole, but recording a series of burial and exposure events could be helpful in archaeological settings, e.g., to constrain multiple construction phases or a series of construction and degradation events. The rocks from MZ005S were collected from a collapsed wall, and the corresponding ages varied between Bronze Age to ⌣200 a. It appears that dating in such a disturbed context provides ages that can be accredited to the initial construction or the subsequent wall degradation. Understanding the archaeological context then becomes invaluable when interpreting such data since rock surface luminescence ages alone cannot differentiate between the initial construction and re-burial during a restoration of the wall. Exposure dating proved less successful than burial dating, with ages being unrealistically young or inconclusive. While our calibration surfaces showed sufficient bleaching, we must conclude that dry-stone structures with luminescence dating might be challenging in alpine areas where rock surfaces are expected to erode. In summary, our work from Val di Sole demonstrates that rock surface luminescence dating of dry-stone walls appears to be a viable method to provide chronological data, which are hard to obtain using other methods.

Declaration of competing interest

The authors declare that they have no known competing financial interests or personal relationships that could have appeared to influence the work reported in this paper.

Acknowledgements

programme (NUAcT). Project ALPES is undertaken in the context of a specific agreement between the Department of Humanities of the University of Trento and the Soprintendenza per i Beni Culturali of the autonomous Province of Trento. The project is funded by the University of Trento, Italy and by the Terre Alte programme of the CAI, Italy (Italian Alpine Club) and is supported by the Municipality of Mezzana, Italy (Trento). The authors are indebted to the people from Ortisé and Menas for their help, and to all the students and researchers who have participated in fieldwork activities. Two reviewers are thanked for their comments, which helped improve the manuscript.

Appendix A. Supplementary data

Supplementary material related to this article can be found online at https://doi.org/10.1016/j.jas.2022.105625.

References

Ageby, L., Angelucci, D.E., Brill, D., Carrer, F., Rades, E.F., Rethemeyer, J., Brückner, H., Klasen, N., 2021. Rock surface IRSL dating of buried cobbles from an alpine dry-stone structure in val di sole, Italy. Quat. Geochronol. 66, 101212. http://dx.doi.org/10.1016/j.quageo.2021.101212.

al Khasawneh, S., Murray, A., Abudanah, F., 2019a. A first radiometric chronology for the khatt shebib megalithic structure in Jordan using the luminescence dating of rock surfaces. Quat. Geochronol. 49, 205–210. http://dx.doi.org/10.1016/j.quageo.2018.02.007.

al Khasawneh, S., Murray, A., Thomsen, K., AbuAzizeh, W., Tarawneh, M., 2019b. Dating a near eastern desert hunting trap (kite) using rock surface luminescence dating. Archaeol. Anthropol. Sci. 11 (5), 2109–2119. http://dx.doi.org/10.1007/s12520-018-0661-3.

Angelucci, D., Carrer, F. (Eds.), 2015. Paesaggi Pastorali d'alta Quota in Val Di Sole (Trento). Le Ricerche Del Progetto ALPES - 2010–2014. Dipartimento di Lettere e Filosofia, Università di Trento, Trento.

Angelucci, D.E., Carrer, F., Ageby, L., Castiglioni, E., Cavulli, F., Dell'Amore, F., Rethemeyer, J., Rottoli, M., Vezzoni, L., Pedrotti, A., 2021. Occupazione pastorale delle alte quote alpine Nell'età Del bronzo: Primi dati dal sito MZ051s (camp da Ortisé, val di sole, Trento). 71, pp. 1–30. http://dx.doi.org/10.32097/1143.

Angelucci, D., Carrer, F., Cavulli, F., 2014. Shaping a periglacial land into a pastoral landscape: A case study from val di sole (Trento, Italy). Eur. J. Post - Class. Archaeol. 4, 157–180.

Angelucci, D., Carrer, F., Pedrotti, A., 2017. Due nuove datazioni dell'età del bronzo da un sito d'alta quota in Val Poré (val di sole).. Archeologia Delle Alpi 154–156.

Bøtter-Jensen, L., Thomsen, K., Jain, M., 2010. Review of optically stimulated luminescence (OSL) instrumental developments for retrospective dosimetry. Radiat. Meas. 45 (3–6), 253–257. http://dx.doi.org/10.1016/j.radmeas.2009.11.030.

Brill, D., Cisternas, M., 2020. Testing quartz and feldspar luminescence dating to determine earthquake and tsunami recurrence in the area of the giant 1960 Chile earthquake. Quat. Geochronol. 58, 101080. http://dx.doi.org/10.1016/j.quageo.2020.101080.

Brill, D., May, S.M., Mhammdi, N., King, G., Lehmann, B., Burow, C., Wolf, D., Zander, A., Brückner, H., 2021. Evaluating optically stimulated luminescence rock surface exposure dating as a novel approach for Reconstructing Coastal boulder movement on decadal to centennial timescales. Earth Surf. Dyn. 9 (2), 205–234. http://dx.doi.org/10.5194/esurf-9-205-2021.

Carrer, F., Angelucci, D.E., 2013. First archaeological data from an alpine pastoral enclosure at val Poré (val di sole, trentino, Italy). Debates Arqueología Medieval 3, 149–165.

Carrer, F., Angelucci, D.E., 2018. Continuity and discontinuity in the history of upland pastoral landscapes: The case study of val molinac and Val Poré (val di sole, Trentino, eastern Italian alps). Landsc. Res. 43 (6), 862–877. http://dx.doi.org/10.1080/01426397.2017.1390078.

Chapot, M.S., Sohbati, R., Murray, A.S., Pederson, J.L., Rittenour, T.M., 2012. Constraining the age of rock art by dating a rockfall event using sediment and rock-surface luminescence dating techniques. Quat. Geochronol. 13, 18–25. http://dx.doi.org/10.1016/j.quageo.2012.08.005.

Colominas, L., Palet, J.M., Garcia-Molsosa, A., 2020. What happened in the highlands? characterising pyrenean livestock practices during the transition from the iron age to the roman period. Archaeol. Anthropol. Sci. 12 (3), 69. http://dx.doi.org/10.1007/s12520-020-01023-3.

Cresswell, A.J., Carter, J., Sanderson, D.C.W., 2018. Dose rate conversion parameters: assessment of nuclear data. Radiat. Meas. 120, 195–201. http://dx.doi.org/10.1016/j.radmeas.2018.02.007.

Dal Piaz, G., Castellarin, A., Martin, S., Selli, L., Carton, A., Pellegrini, G., Casolari, E., Daminato, F., Picotti, V., Prosser, G., Santulana, E., Cantelly, L., 2007. Carta geologica d'Italia alla scala 1:50.000. foglio 042. Malé + note illustrative della carta geologica d'Italia alla scala 1:50.000.

Dell'Amore, F., Carrer, F., Angelucci, D., 2017. Reperti Archeologici Dalla Val Molinac E Dalla Val Poré (Val Di Sole, Trento, Italia).

Favilli, F., Egli, M., Brandova, D., Ivy-Ochs, S., Kubik, P.W., Maisch, M., Cherubini, P., Haeberli, W., 2009. Combination of numerical dating techniques using ^{10}Be in rock boulders and ^{14}C of resilient soil organic matter for reconstructing the chronology of glacial and periglacial processes in a high alpine catchment during the late pleistocene and early holocene. Radiocarbon 51 (2), 537–552. http://dx.doi.org/10.1017/S0033822200055910.

Ferrater, M., Silva, P.G., Ortuño, M., Rodríguez-Pascua, M.A., Masana, E., 2015. Archaeoseismological analysis of a late bronze age site on the alhama de murcia fault, SE Spain. Geoarchaeology 30 (2), 151–164. http://dx.doi.org/10.1002/gea.21505.

Freiesleben, T., Sohbati, R., Murray, A., Jain, M., al Khasawneh, S., Hvidt, S., Jakobsen, B., 2015. Mathematical model quantifies multiple daylight exposure and burial events for rock surfaces using luminescence dating. Radiat. Meas. 81, 16–22. http://dx.doi.org/10.1016/j.radmeas.2015.02.004.

Galli, A., Panzeri, L., Rondini, P., Poggiani Keller, R., Martini, M., 2020. Luminescence dating of rock surface. the case of monoliths from the megalithic sanctuary of ossimo-pat (Valle Camonica, Italy). Appl. Sci. 10 (21), 7403. http://dx.doi.org/10.3390/app10217403.

Gliganic, L.A., Meyer, M.C., May, J.-H., Aldenderfer, M.S., Tropper, P., 2021. Direct dating of lithic surface artifacts using luminescence. Sci. Adv. 7 (23), eabb3424. http://dx.doi.org/10.1126/sciadv.abb3424.

Gliganic, L.A., Meyer, M.C., Sohbati, R., Jain, M., Barrett, S., 2019. OSL surface exposure dating of a lithic quarry in tibet: laboratory validation and application. Quat. Geochronol. 49, 199–204. http://dx.doi.org/10.1016/j.quageo.2018.04.012.

Greilich, S., Glasmacher, U.A., Wagner, G.A., 2005. Optical dating of granitic stone surfaces. Archaeometry 47 (3), 645–665. http://dx.doi.org/10.1111/j.1475-4754.2005.00224.x.

Habermann, J., Schilles, T., Kalchgruber, R., Wagner, G.A., 2000. Steps towards surface dating using luminescence. Radiat. Meas. 32 (5), 847–851. http://dx.doi.org/10.1016/S1350-4487(00)00066-4.

Harris, E.C. (Ed.), 1989. Principles of archaeological stratigraphy (second edition). Academic Press, London, http://dx.doi.org/10.1016/B978-0-12-326651-4.50001-8.

Holl, A.F.C., 1998. Livestock husbandry, pastoralisms, and territoriality: the west african record. J. Anthropol. Archaeol. 17 (2), 143–165. http://dx.doi.org/10.1006/jaar.1998.0321.

Huntley, D.J., Lamothe, M., 2001. Ubiquity of anomalous fading in K-feldspars and the measurement and correction for it in optical dating. Can. J. Earth Sci. 38 (7), 1093–1106. http://dx.doi.org/10.1139/e01-013.

Ilves, K., 2018. Stone foundation houses of the late iron age and early medieval Å land and new C14-dates from the settlment of kulla. Fennoscandia Archaeol. XXXIV, 59–82.

Ishii, Y., Takahashi, T., Ito, K., 2022. Luminescence dating of cobbles from pleistocene fluvial terrace deposits of the Ara River, Japan. Quat. Geochronol. 67, 101228. http://dx.doi.org/10.1016/j.quageo.2021.101228.

Jaubert, J., Verheyden, S., Genty, D., Soulier, M., Cheng, H., Blamart, D., Burlet, C., Camus, H., Delaby, S., Deldicque, D., Edwards, R.L., Ferrier, C., Lacrampe-Cuyaubère, F., Lévêque, F., Maksud, F., Mora, P., Muth, X., Régnier, E., Rouzaud, J.-N., Santos, F., 2016. Early neanderthal constructions deep in bruniquel cave in southwestern France. Nature 534 (7605), 111–114. http://dx.doi.org/10.1038/nature18291.

Jenkins, G.T.H., Duller, G.A.T., Roberts, H.M., Chiverrell, R.C., Glasser, N.F., 2018. A new approach for luminescence dating glaciofluvial deposits - high precision optical dating of cobbles. Quat. Sci. Rev. 192, 263–273. http://dx.doi.org/10.1016/j.quascirev.2018.05.036.

Junge, A., Lomax, J., Shahack-Gross, R., Dunseth, Z.C., Finkelstein, I., Fuchs, M., 2016. OSL age determination of archaeological stone structures using trapped aeolian sediments: A case study from the negev highlands, Israel. Geoarchaeology 31 (6), 550–563. http://dx.doi.org/10.1002/gea.21578.

Kemp, J., Olley, J., Stout, J., Pietsch, T., Corporation, M.A., 2022. Dating stone arrangements using optically stimulated luminescence and fallout radionuclides. Geoarchaeology n/a (n/a), 1–11. http://dx.doi.org/10.1002/gea.21902.

Kremenić, T., Andlar, G., Varotto, M., 2021. How did sheep save the day? the role of dry stone wall heritage and agropastorality in historical landscape preservation. A case-study of the town of cres olive grove. Land 10 (9), 978. http://dx.doi.org/10.3390/land10090978.

Kreutzer, S., Burow, C., Dietze, M., Fuchs, M.C., Schmidt, C., Fischer, M., Friedrich, J., Mercier, N., Smedley, R.K., Christophe, C., Zink, A., Durcan, J., King, G.E., Philippe, A., Guerin, G., Riedesel, S., Autzen, M., Guibert, P., Mittelstrass, D., Gray, H.J., Fuchs, M., 2021. Luminescence: comprehensive luminescence dating data analysis.

Laskaris, N., Liritzis, I., 2011. A new mathematical approximation of sunlight attenuation in rocks for surface luminescence dating. J. Lumin. 131 (9), 1874–1884. http://dx.doi.org/10.1016/j.jlumin.2011.04.052.

Lehmann, B., Herman, F., Valla, P.G., King, G.E., Biswas, R.H., 2019a. Evaluating post-glacial bedrock erosion and surface exposure duration by coupling in situ optically stimulated luminescence and ^{10}Be dating. Earth Surf. Dyn. 7 (3), 633–662. http://dx.doi.org/10.5194/esurf-7-633-2019.

Lehmann, B., Herman, F., Valla, P.G., King, G.E., Biswas, R.H., Ivy-Ochs, S., Steinemann, O., Christl, M., 2019b. Postglacial erosion of bedrock surfaces and deglaciation timing: new insights from the mont blanc massif (western alps). Geology 48 (2), 139–144. http://dx.doi.org/10.1130/G46585.1.

Lehmann, B., Valla, P.G., King, G.E., Herman, F., 2018. Investigation of OSL surface exposure dating to reconstruct post-LIA glacier fluctuations in the French Alps (mer de glace, mont blanc massif). Quat. Geochronol. 44, 63–74. http://dx.doi.org/10.1016/j.quageo.2017.12.002.

Levine, E.I., Rothenberg, M.A.W., Siegel, O., Knoblauch, C., Bestock, L., Klein, L., 2019. The uronarti regional archaeological project: second cataract fortresses and the western desert of Sudan. Antiquity 93 (372), http://dx.doi.org/10.15184/aqy.2019.183.

Liritzis, I., 2001. Searching for precision of a new "luminescence clock" in dating calcitic rocks. J. Radioanal. Nucl. Chem. 247 (3), 727–730. http://dx.doi.org/10.1023/A:1010696308875.

Liritzis, I., Aravantinos, V., Polymeris, G.S., Zacharias, N., Fappas, I., Agiamarniotis, G., Sfampa, I.K., Vafiadou, A., Kitis, G., 2015. Witnessing prehistoric delphi by luminescence dating. C. R. Palevol 14 (3), 219–232. http://dx.doi.org/10.1016/j.crpv.2014.12.007.

Liritzis, I., Bednarik, R.G., Kumar, G., Polymeris, G., Iliopoulos, I., Xanthopoulou, V., Zacharias, N., Vafiadou, A., Bratitsi, M., 2019a. Daraki-chattan rock art constrained OSL chronology and multianalytical techniques: A first pilot investigation. J. Cult. Herit. 37, 29–43. http://dx.doi.org/10.1016/j.culher.2018.09.018.

Liritzis, I., Panou, E., Exarhos, M., 2017. Novel Approaches In Surface Luminescence Dating Of Rock Art: A Brief Review. Zenodo, http://dx.doi.org/10.5281/ZENODO.893194.

Liritzis, I., Polymeris, G.S., Vafiadou, A., Sideris, A., Levy, T.E., 2019b. Luminescence dating of stone wall, tomb and ceramics of kastrouli (phokis, Greece) late helladic settlement: case study. J. Cult. Herit. 35, 76–85. http://dx.doi.org/10.1016/j.culher.2018.07.009.

Liritzis, I., Vafiadou, A., 2015. Surface luminescence dating of some Egyptian monuments. J. Cult. Herit. 16 (2), 134–150. http://dx.doi.org/10.1016/j.culher.2014.05.007.

Liritzis, I., Zacharias, N., Al-Otaibi, F., Iliopoulos, I., Katagas, C., Shaltout, M., 2016. Chronology of construction and occupational phases of nawamis tombs, sinai based on OSL dating. Geochronometria 43, http://dx.doi.org/10.1515/geochr-2015-0041.

Liritzis, I., Zacharias, N., Polymeris, G.S., 2010. Surface luminescence dating of 'dragon houses' and armena gate at styra (euboea, Greece). Mediterr. Archaeol. Archaeom. 10 (3), 65–81.

Liszka, K., 2017. Egyptian or nubian? dry-stone architecture at wadi el-hudi, wadi es-sebua, and the eastern desert. J. Egypt. Archaeol. 103 (1), 35–51. http://dx.doi.org/10.1177/0307513317714407.

Manley, J., 1990. A late bronze age landscape on the denbigh moors, northeast Wales. Antiquity 64 (244), 514–526. http://dx.doi.org/10.1017/S0003598X00078418.

Mazet, S., 2006. Habitat and stone enclosure of corsica: what is the function of the enclosed area during the neolithic and the bronze age? In: 2006 First International Symposium on Environment Identities and Mediterranean Area. http://dx.doi.org/10.1109/ISEIMA.2006.345020.

Medici, T., Foradori, G., Carrer, F., Maschio, R., Gialanella, S., Montagna, M., Pedrotti, A., Angelucci, D., 2014. Una perlina in vetro da un contesto pastorale d'altura della val di sole (trento). ISBN: 978-88-907297-3-7, pp. 115–123.

Meyer, M., Gliganic, L., Jain, M., Sohbati, R., Schmidmair, D., 2018. Lithological controls on light penetration into rock surfaces – implications for OSL and IRSL surface exposure dating. Radiat. Meas. 120, 298–304. http://dx.doi.org/10.1016/j.radmeas.2018.03.004.

Murray, A.S., Marten, R., Johnston, A., Martin, P., 1987. Analysis for naturally occuring radionuclides at environmental concentrations by Gamma spectrometry. J. Radioanal. Nucl. Chem. Artic. 115 (2), 263–288. http://dx.doi.org/10.1007/BF02037443.

Murray, A., Wintle, A., 2000. Luminescence dating of quartz using an improved single-aliquot regenerative-dose protocol. Radiat. Meas. 32 (1), 57–73. http://dx.doi.org/10.1016/S1350-4487(99)00253-X.

Ou, X., Roberts, H., Duller, G., Gunn, M., Perkins, W., 2018. Attenuation of light in different rock types and implications for rock surface luminescence dating. Radiat. Meas. 120, 305–311. http://dx.doi.org/10.1016/j.radmeas.2018.06.027.

Passariello, I., Talamo, P., D'Onofrio, A., Barta, P., Lubritto, C., Terrasi, F., 2010. Contribution of radiocarbon dating to the chronology of eneolithic in campania (Italy). GEOCHR 35 (-1), 25–33. http://dx.doi.org/10.2478/v10003-010-0008-2.

Polikreti, K., Michael, C., Maniatis, Y., 2002. Authenticating marble sculpture with thermoluminescence. Ancient TL 20, 11–18.

Prescott, J.R., Hutton, J.T., 1994. Cosmic ray contributions to dose rates for luminescence and ESR dating: large depths and long-term time variations. Radiat. Meas. 23 (2), 497–500. http://dx.doi.org/10.1016/1350-4487(94)90086-8.

Rades, E., Sohbati, R., Lüthgens, C., Jain, M., Murray, A., 2018. First luminescence-depth profiles from boulders from moraine deposits: insights into glaciation chronology and transport dynamics in malta valley, Austria. Radiat. Meas. 120, 281–289. http://dx.doi.org/10.1016/j.radmeas.2018.08.011.

Reimann, T., Tsukamoto, S., Naumann, M., Frechen, M., 2011. The potential of using K-rich feldspars for optical dating of Young coastal sediments – A test case from darss-zingst peninsula (southern baltic sea coast). Quat. Geochronol. 6 (2), 207–222. http://dx.doi.org/10.1016/j.quageo.2010.10.001.

Reitmaier, T., Lambers, K., Walser, C., Zingman, I., Haas, J.N., Dietre, B., Reidl, D., Hajdas, I., Nicolussi, K., Kathrein, Y., Naef, L., Kaiser, T., 2013. Alpine Archäologie in der silvretta. Archäologie Schweiz 36 (1), 4–15.

Riedesel, S., Autzen, M., 2020. Beta and Gamma dose rate attenuation in rocks and sediment. Radiat. Meas. 133, 106295. http://dx.doi.org/10.1016/j.radmeas.2020.106295.

Riedesel, S., Autzen, M., 2021. Calc_CobbleDoseRate: calculate dose rate of slices in a spherical cobble.

Sohbati, R., Murray, A.S., Buylaert, J.P., Almeida, N.A.C., Cunha, P.P., 2012a. Optically stimulated luminescence (OSL) dating of quartzite cobbles from the tapada do montinho archaeological site (east-central Portugal): OSL dating of quartzite cobbles, tapada do montinho, Portugal. Boreas 41 (3), 452–462. http://dx.doi.org/10.1111/j.1502-3885.2012.00249.x.

Sohbati, R., Murray, A.S., Chapot, M.S., Jain, M., Pederson, J., 2012b. Optically stimulated luminescence (OSL) as a chronometer for surface exposure dating. J. Geophys. Res.: Solid Earth 117 (B9), http://dx.doi.org/10.1029/2012JB009383.

Sohbati, R., Murray, A.S., Jain, M., Buylaert, J.P., Thomsen, K.J., 2011. Investigating the resetting of OSL signals in rock surfaces. Geochronometria 38 (3), 249–258. http://dx.doi.org/10.2478/s13386-011-0029-2.

Sohbati, R., Murray, A.S., Porat, N., Jain, M., Avner, U., 2015. Age of a prehistoric "Rodedian" cult site constrained by sediment and rock surface luminescence dating techniques. Quat. Geochronol. 30, 90–99. http://dx.doi.org/10.1016/j.quageo.2015.09.002.

Souza, P.E., Sohbati, R., Murray, A.S., Clemmensen, L.B., Kroon, A., Nielsen, L., 2021. Optical dating of cobble surfaces determines the chronology of holocene beach ridges in Greenland. Boreas 50 (2), 606–618. http://dx.doi.org/10.1111/bor.12507.

Souza, P.E., Sohbati, R., Murray, A.S., Kroon, A., Clemmensen, L.B., Hede, M.U., Nielsen, L., 2019. Luminescence dating of buried cobble surfaces from sandy beach ridges: A case study from Denmark. Boreas 48 (4), 841–855. http://dx.doi.org/10.1111/bor.12402.

Team, R.C., 2021. R: A Language and Environment for Statistical Computing. R Foundation for Statistical Computing, Vienna, Austria, URL https://www.R-project.org/.

Thomsen, K.J., Murray, A.S., Jain, M., Bøtter-Jensen, L., 2008. Laboratory fading rates of various luminescence signals from feldspar-rich sediment extracts. Radiat. Meas. 43 (9), 1474–1486. http://dx.doi.org/10.1016/j.radmeas.2008.06.002.

Vafiadou, A., Murray, A., Liritzis, I., 2007. Optically stimulated luminescence (OSL) dating investigations of rock and underlying soil from three case studies. J. Archaeol. Sci. 34 (10), 1659–1669. http://dx.doi.org/10.1016/j.jas.2006.12.004.

Walsh, K., 2005. Risk and marginality at high altitudes: new interpretations from fieldwork on the faravel plateau, hautes-alpes. Antiquity 79, http://dx.doi.org/10.1017/S0003598X00114097.

Walsh, K., Court-Picon, M., de Beaulieu, J.-L., Guiter, F., Mocci, F., Richer, S., Sinet, R., Talon, B., Tzortzis, S., 2014. A historical ecology of the ecrins (southern french alps): archaeology and palaeoecology of the mesolithic to the medieval period. Quat. Int. 353, 52–73. http://dx.doi.org/10.1016/j.quaint.2013.08.060.

Yar, B., Dubois, P., 1996. Les structures d'habitat au Paléolithique inférieur et moyen en France : entre réalité et imaginaire. Bull. Société Préhistorique Française 93 (2), 149–163. http://dx.doi.org/10.3406/bspf.1996.10133.